石油技術協会誌　第 70 巻　第 5 号（平成 17 年 9 月）
JOURNAL OF THE JAPANESE ASSOCIATION FOR PETROLEUM TECHNOLOGY
VOL. 70, NO. 5 (Sept., 2005)

論　　文

A fundamental study of microbial attachment and transport in porous media for the design of MEOR*

Yan-Guo Yang**, Yuichi Niibori***, Chihiro Inoue**** and Tadashi Chida****

(Received April 5, 2005；Accepted July 8, 2005)

Abstract：　Generally, the cell number of the microbes attaching to the solid phase is large rather than that of microbes floating in the pores. For more reliable MEOR (Microbial Enhanced Oil Recovery), such attachment microbes should be distributed efficiently in the target zone of reservoir. In order to understand the attachment behavior of microbes in the flow system of porous media, in this study the relation of the attachment amount and the fluid flow velocity has been examined using a vertical, two-dimensional packed bed (plate-type packed bed).

Lactobacillus casei (IFO 15883) was used as the test microbe in this study. The microbe exhibits no motility or chemotaxis and does not produce gas. In the experiments, the growth rate of the microbe was negligible small by controlling the nutrients. The concentration of the cell suspension out of the bed was traced by the turbidity of the suspension. Then, the change of the concentration was analyzed by two-dimensional, advection-dispersion model with the attachment/detachment rate of microbes.

For the experimental results, this study evaluated W_{out}/W_{in} as the cell recovery, where W_{out} is the cell number flowed out of the packed bed, and W_{in} is the total cell number inputted into the packed bed. Also the maximum attachment amount based on the Langmuir type equation was estimated through the analysis by the two-dimensional mathematical model. The cell recovery and the maximum attachment amount strongly depended on both the injection concentration of the cell suspension, $c_{b_{in}}$, and the injection flow velocity into the packed bed, v_{in}. The experimental results showed an optimal value of the ratio of $c_{b_{in}}$ to v_{in}, for both the maximum attachment amount and the cell recovery. The optimal value does not always agree with that obtained from one-dimensional packed bed.

Key words：　MEOR, Cell recovery, Cell attachment amount, Two-dimensional porous media.

1. Introduction

MEOR (Microbial Enhanced Oil Recovery) is expected to induce various functions such as reservoir repressurization, interfacial tension/oil viscosity reduction, and selective plugging of the most permeable zones[1]. Therefore, the dynamic behaviors of microbes applied to the target zones of reservoir are very complicated. However, for more reliable design of MEOR, we must understand and control the detail of the distribution of microbes in such a reservoir. Particularly, since the amount of cell attachment on the solid surface is larger than that floating in pores[2], the microbial attachment process is considered as one of the central issues.

So far, the application of indigenous or exogenous microbes to the subsurface system has been discussed for not only MEOR[3], but also bioremediation[4),5]. Through such various approaches, the adsorption rate equations of the Langmuir type is widely used for determining the attachment/detachment or clogging/declogging rates of microbes in porous media[6-10]. In addition, amount of experiments and modeling of

* 平成 12 年 5 月 25 日，平成 12 年度石油技術協会春季講演会 開発・生産部門個人講演で一部講演　A part of this paper was presented at the 2000 JAPT Spring Meeting held in Niigata, May 25, 2000.

** 東北大学大学院環境科学研究科 Graduate School of Environment Study, Tohoku University (現在，日本リファイン㈱　NIPPON REFINE CO., LTD.)
*** 東北大学大学院工学研究科　Graduate School of Engineering, Tohoku University
**** 東北大学大学院環境科学研究科　Graduate School of Environment Study, Tohoku University

microbial transport were reported[11-15]. Most of these mathematical models are one-dimensional (vertical or horizontal), although Shonnard *et al.*[16] investigated the transport and attachment of microbes using a two-dimensional sand-filled aquifer simulator. Nevertheless, the difference between one-dimensional and two-dimensional approaches has not been discussed sufficiently.

This study focuses on the relation of the attachment amount and the fluid flow velocity, based on laboratory experiments using a vertical, plate-type (two-dimensional) packed bed with glass beads. In the experiments, *Lactobacillus casei* (IFO 15883) was used as the test microbe. Since the microbe produces no gas, and has no motility or chemotaxis, we can examine the attachment and detachment phenomena of the microbes and the local density difference of the cell suspension in the packed bed. To explain the transport of microbes in the porous media, a two-dimensional mathematical model is used, in which the gravitation and the attachment/detachment phenomena of microbes are considered. From the best fit of the numerical calculations to the experimental data, this study evaluated the apparent maximum-attachment-amount defined by the Langmuir type equation. The concentration of cell (microbe) flowing out of the packed bed and the maximum attachment amount strongly depended on both the injection concentration of the cell suspension, $c_{b_{in}}$, and the injection flow velocity into the packed bed, v_{in}.

2. Experimental

2.1 Microbes and growth conditions

As the test microbe, we selected *Lactobacillus casei* (Institute for Fermentation, Osaka Culture Collection of Microorganisms: IFO 15883). The microbe can grow under either aerobic or anaerobic conditions, converts glucose (substrate) only to lactic acid while producing no gas, and exhibits no motility or chemotaxis. Their size is around 1 micrometer in diameter, and 2 micrometer in length, as shown in Fig. 1. The medium (IFO 804 medium) consisted of 5 g-glucose, 5 g-yeast extract, 5 g-polypepton and 1 g-$MgSO_4 \cdot 7H_2O$ per liter of distilled water, and was autoclaved in advance. The cells were collected by centrifugation after incubating at 30℃ for more than

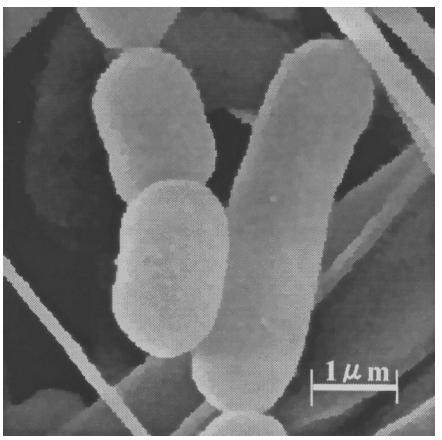

Fig. 1 SEM image of *Lactobacillus casei* (IFO 15883)

48 hours in the medium. The cell pellet was washed once in distilled water, and the cells were resuspended in distilled water. For some experiments, 5 (wt) % of the supernatant after centrifugation of culture was added to the cell suspensions, in order to imitate the circumstances of microbial transport.

Fig. 2 shows the changes in cell concentration with time. In these experiments, the cells were suspended in distilled water only or in distilled water containing 5 (wt) % supernatant. As shown in Fig. 2, we can ignore the growth or death of the microbe at least within 6 hours for each case, even if the supernatant is added into the cell suspension.

The concentration of the cell suspension flowing out of the packed beds was determined by the turbidity of the suspension at the wavelength of 600nm. When the

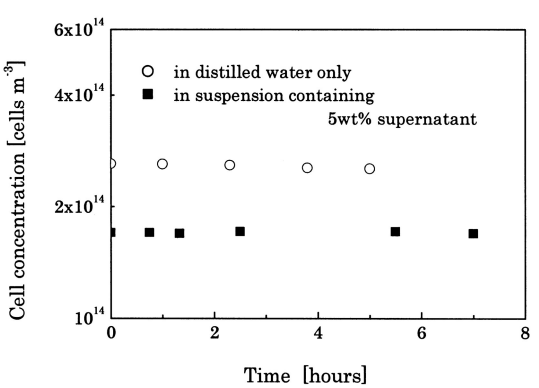

Fig. 2 Behaviors of *Lactobacillus casei* in distilled water only (○, the initial concentration was 2.6×10^{14} cells m^{-3}), and that containing the 5 (wt) % supernatant. (■, the initial concentration was 1.7×10^{-14} cell m^{-3}.)

concentration was greater than 2.7×10^{-14} cells m^{-3}, the turbidity was measured after dilution with distilled water containing 5 (wt) % supernatant, so that the turbidity remained in the range where the cell concentration is linear as a function of the turbidity.

2.2 Breakthrough experiments

Fig. 3 shows a schematic diagram of the experimental process and the two-dimensional (2D) packed bed. After inputting the predetermined volume of the cell suspension for a particular condition as shown in Table 1, distilled water was allowed to flow into the bed and the turbidity of the outflow fluid was monitored for a given time period (until 4 in pore volume). Two peristaltic pumps were used to separately input the cell suspension and the distilled water. The packed bed with glass beads (1 mm diameter) was 10 mm in thickness, 0.15 m in height and 0.60 m in length, and its pore volume and permeability were about 3.6×10^{-4} m^3 (the porosity was about 40%) and 8.20×10^{-10} m^2, respectively. To input and output the cell suspension at a uniform fluid velocity at both edges of the bed, two acrylic tubes (8 mm inner diameter) with openings of 1 mm diameter every 10 mm were installed along the input and the output lines. In order to prevent the outflow of glass beads through these openings, each was covered inside with a 100-mesh net. Moreover, to maintain uniform porosity of the bed, silicone gum-sheets of 0.5 mm

Table 1 Experimental condition

Run number	Input conditions*	
	Cell-input concentration [10^{14} cells m^{-3}]	Flow velocity [m s^{-1}]
B-44	2.4	3.20×10^{-5}
B-54	2.4	6.50×10^{-5}
B-53	2.4	13.0×10^{-5}
B-55	4.4	3.20×10^{-5}
B-17	6.4	6.50×10^{-5}

*: The input time of the cell suspension was always fixed at 1 in the pore volume of packed bed.

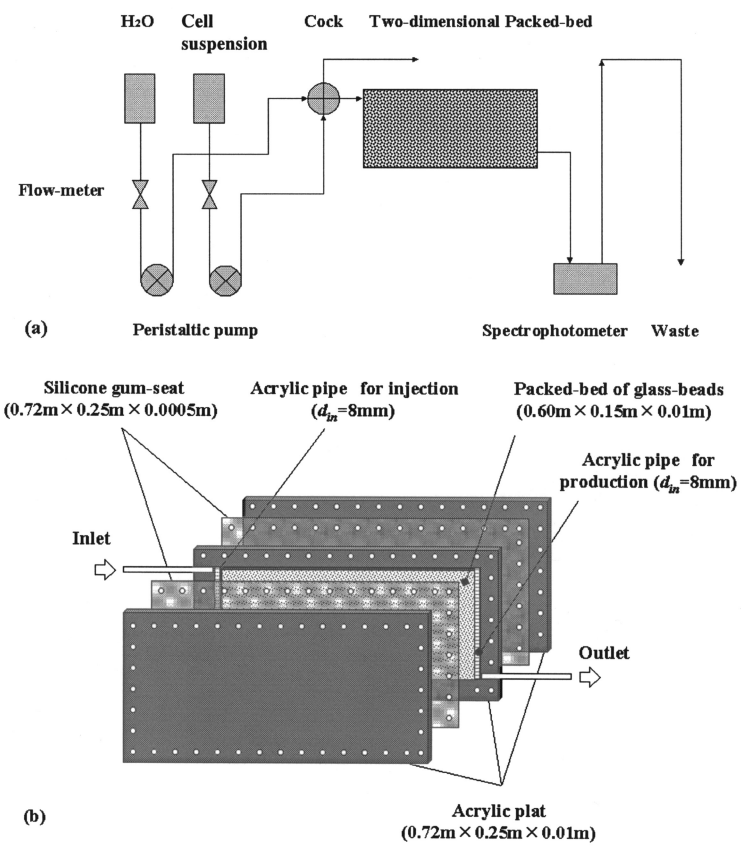

Fig. 3 Schematic diagram of experimental process (a), and the 2D packed bed (b).

thickness were placed on each acrylic plate, as shown in Fig. 3 (b). In the experimental conditions of Table 1, the cell-input concentrations were in the order of 10^{14} cells m^{-3} (i.e., 10^8 cells/ml). These values are in the range of maximum concentration of a microbe (from 10^{14} cells m^{-3} to 10^{15} cells m^{-3}) for a practical MEOR already reported by Sugai *et al.*[17),18)] and Yonebayashi *et al.*[19)].

3. Mathematical model

3.1 Mass balance equation and the continuous equation

In addition to advection and hydrodynamic dispersion, the attachment/detachment, motility and chemotaxis of microbes must be also considered in order to explain the transport of microbes in saturated porous media. In the duration of this study, the growth or death of microbe during the experiment can be neglected, because the cell concentration in the suspension did not change, as shown in Fig. 2. In addition, the major assumptions for the mathematical model are as follows:

a. a porous medium is saturated with water,
b. the permeability and the porosity of the porous medium are homogeneous and isotropic,
c. the decrease in pore volume due to cell attachment on the solid phase can be neglected,
d. the densities, except in gravitational terms, are constant (Boussinesq's approximation), and
e. the fluid in which the cells are suspended is incompressible.

Based on these assumptions, we can obtain the following equations:

$$\theta\left(\frac{\partial c_b}{\partial t}+\frac{\partial c_s}{\partial t}\right)=\frac{\partial}{\partial x}\left(\theta D_{ex}\frac{\partial c_b}{\partial x}\right)+\frac{\partial}{\partial z}\left(\theta D_{ez}\frac{\partial c_b}{\partial z}\right)-\left(\frac{\partial (v_x c_b)}{\partial x}+\frac{\partial (v_z c_b)}{\partial z}\right), \quad (1)$$

$$\frac{\partial v_x}{\partial x}+\frac{\partial v_z}{\partial z}=0 , \quad (2)$$

where t is time [s], x and z are the horizontal and vertical coordinates [m], respectively, c_b is the cell concentration in the suspension [cells m^{-3}], c_s is the concentration of microbes attached on the solid phase (defined as the number of microbes attached per unit pore volume) [cells m^{-3}], θ is the porosity of the packed bed [m^3 m^{-3}], D_e is the effective dispersion coefficient [m^2 s^{-1}], and v is the Darcy flow velocity [m s^{-1}]. The suffixes, x and z, indicate the $x-$ and $z-$ directions, respectively.

Considering the finite number of retaining sites of porous medium for microbes, Corapcioglu and Haridas[20-21)] and Tan *et al.*[8)] proposed the following kinetic equation describing the attachment and detachment of microbes in porous media.

$$\frac{\partial c_s}{\partial t}=k_a\frac{c_{smax}-c_s}{c_{smax}}c_b-k_y c_s , \quad (3)$$

where k_a and k_y are the attachment and detachment rate-coefficients [s^{-1}] (including a conversion coefficient about porosity, $(1-\theta)/\theta$), respectively, and c_{smax} is the maximum retention capacity [cells m^{-3}]. Also in this study, this kinetic model is used to examine the transport and distribution of microbes in two-dimensional porous media.

Based on Darcy's law, the velocities shown in equation (1) and (2) are described by

$$v_x=-\frac{k}{\mu}\frac{\partial p}{\partial x} , \quad (4)$$

$$v_z=-\frac{k}{\mu}\left(\frac{\partial p}{\partial z}+\rho g\right) , \quad (5)$$

where k is the permeability [m^2], p is the pressure [Pa], μ is the viscosity of the fluid [Pa s], ρ is the density of the cell suspension [kg m^{-3}] and g is the gravitational acceleration [m s^{-2}]. The change in the fluid density with the cell concentration is described by

$$\beta=\frac{1}{\rho}\frac{\partial \rho}{\partial c_b} , \quad (6)$$

where β is the expansion coefficient of fluid [m^3 $cells^{-1}$]. We can solve this equation using the Taylor expansion. Disregarding the terms of higher orders than the second term in the Taylor expansion series, the density is yielded by

$$\rho=\rho_0\{1+\beta(c_b-c_{bin})\} , \quad (7)$$

where ρ_0 and c_{bin} are the density [kg m^{-3}] and the cell-input concentration [cells m^{-3}] in the suspension, respectively.

3.2 Initial and boundary conditions

The initial and the boundary conditions are given as follows:

$$c_b = 0,\ c_s = 0,\ \text{at}\ t = 0,$$

$$\frac{\partial c_b}{\partial z} = 0,\ \frac{\partial v_x}{\partial z} = 0,\ v_z = 0,\ \text{at}\ z = 0$$

$$\text{and}\ z = z_1\ (0 < x < x_1),$$

$$\left(-\theta D_{ex}\frac{\partial c_b}{\partial x} + v_{in}c_b\right)\Big|_{x=0+} = v_{in}c'_{b_{in}},\ v_x = v_{in},$$

$$v_z = 0,\ \text{at}\ x = 0\ (0 \le z \le z_1),$$

$$(c'_{b_{in}} = c_{b_{in}}\ \textit{when}\ 0 \le t \le t_{in}$$

$$\textit{and}\ \ c'_{b_{in}} = 0\ \textit{when}\ t > t_{in})$$

$$\frac{\partial c_b}{\partial x} = 0,\ v_x = v_{in},\ v_z = 0,$$

$$\text{at}\ x = x_1\ (0 \le z \le z_1), \tag{8}$$

where x_1 and z_1 are the length and height of the packed bed [m], respectively, and v_{in} is the input flow velocity [m s^{-1}].

Further, we assume that the difference between the horizontal and the vertical dispersion coefficient is negligibly small compared to the degree of the advection term in microbial transport[22]. Then, we define the following dimensionless variables and parameters:

$$X = \frac{x}{x_1},\ Z = \frac{z}{x_1},\ V_x = \frac{v_x}{v_{in}},$$

$$V_z = \frac{v_z}{v_{in}},\ T = \frac{tv_{in}}{x_1\theta},$$

$$C_b = \frac{c_b}{c_{b_{in}}},\ C_s = \frac{c_s}{c_{b_{in}}},\ C_{smax} = \frac{c_{smax}}{c_{b_{in}}},$$

$$K_a = \frac{x_1\theta}{v_{in}}k_a,\ K_y = \frac{x_1\theta}{v_{in}}k_y,$$

$$\textit{and}\ p_e = \frac{v_{in}x_1}{D_e\theta} \tag{9a}$$

$$R_a = \frac{kg\rho_0\beta c_{b_{in}}}{v_{in}\mu}, \tag{9b}$$

where P_e and R_a are the Peclet number and the Rayleigh number, respectively. As the stream function, Ψ,

$$V_x = \frac{\partial\Psi}{\partial Z}\ \text{and}\ V_z = -\frac{\partial\Psi}{\partial X}, \tag{10}$$

are defined, the dimensionless fundamental equations can be described as

$$\frac{\partial C_b}{\partial T} + \frac{\partial C_s}{\partial T} = \frac{1}{P_e}\left(\frac{\partial^2 C_b}{\partial X^2} + \frac{\partial^2 C_b}{\partial Z^2}\right) - \left(V_x\frac{\partial C_b}{\partial X} + V_z\frac{\partial C_b}{\partial Z}\right), \tag{11}$$

$$\frac{\partial^2\Psi}{\partial X^2} + \frac{\partial^2\Psi}{\partial Z^2} = R_a\frac{\partial C_b}{\partial X}, \tag{12}$$

$$\frac{\partial C_s}{\partial T} = K_a\frac{C_{smax} - C_s}{C_{smax}}C_b - K_yC_s,$$

$$\frac{\partial C_b}{\partial Z} = 0,\ \frac{\partial V_x}{\partial Z} = 0,\ V_z = 0,$$

$$\text{at}\ Z = 0\ \textit{and}\ Z = Z_1\ (0 < X < 1), \tag{13}$$

$$\left(-\frac{1}{P_e}\frac{\partial C_b}{\partial X} + V_{in}C_b\right)\Big|_{X=0+} = V_{in}C'_{b_{in}},\ V_x = V_{in},$$

$$V_z = 0,\ \text{at}\ X = 0\ (0 \le Z \le Z_1),$$

$$(C'_{b_{in}} = C_{b_{in}}\ \textit{when}\ 0 \le T \le T_{in}$$

$$\textit{and}\ C'_{b_{in}} = 0\ \textit{when}\ T > T_{in}),$$

$$\frac{\partial C_b}{\partial X} = 0,\ V_x = V_{in},\ V_z = 0,$$

$$\text{at}\ X = 1\ (0 \le Z \le Z_1). \tag{14}$$

The above dimensionless equations were numerically solved using the finite difference method combined with the explicit scheme. To avoid error originating from the numerical dispersion, the three-order upwind formula[23] was applied to the first-order spatial derivative corresponding to the convection term, i.e.,

$$\left(\frac{\partial C_b}{\partial X}\right)_{i,j} = \frac{C_{b_{i-2,j}} - 6C_{b_{i-1,j}} + 3C_{b_{i,j}} + 2C_{b_{i+1,j}}}{6\Delta X}, \tag{15}$$

where the suffixes, i and j, are the counters of grid in the numerical calculation, and ΔX is the discrete distance in X-direction.

3.3 Parameters estimation

The hydrodynamic dispersion coefficient was estimated using the 2D horizontal packed bed. Since the Rayleigh number, R_a, defined in equation (9b), can be assumed to be zero in the horizontal flow, we can apply the one-dimensional advection-dispersion model to the breakthrough data. In the results, the dispersion coefficient was evaluated to be 7.8×10^{-6} m^{2}s^{-1} at the

flow velocity of 6.5×10^{-5} m s^{-1}. In the flow velocity range from 3.2×10^{-5} m s^{-1} to 1.3×10^{-4} m s^{-1} in this study, the dispersion coefficient is proportional to the flow velocity, as shown by Levenspiel[24], and Tan *et al.*[8]. Therefore, the Peclet number, P_e, can be estimated to be around 50 for the packed bed used in this study. This value agrees reasonably well with the Peclet number evaluated by Tan *et al.*[8], who conducted a one-dimensional experiment using a column packed with sand (90.3% of the sand particle were 0.5 through 2.0 mm in size).

In the 2D vertical packed bed, the Rayleigh number, R_a, takes a value greater than zero. To calculate its value, we need the values of the parameters included in equation (9b), such as β, μ and ρ_0. Based on the equation (7) and the correlation between the cell concentration and the density of the cell suspension, the value of the expansion coefficient of fluid, β, was estimated to be 1.675×10^{-18} m^3 cells^{-1}. Further, by using the following values, the fluid viscosity μ of 0.89×10^{-3} Pa s, the density of cell suspension ρ_0 of 1.0×10^3 kg m^{-3}, the permeability k of 8.20×10^{-10} m^2 of the packed bed and the gravitational acceleration g of 9.8 m s^{-2}, the practical values of the Rayleigh number were evaluated. The attachment and the detachment rate-coefficients, k_a and k_y, and the maximum retention capacity $c_{s_{max}}$ were adjusted to obtain the best fit of the numerical calculation to the experimental data.

4. Results and discussion

Fig. 4 shows the experimental data and the numerical results calculated based on the two-dimensional mathematical model (where solid line, dotted line and broken line in the figures are the calculated results). Table 2 shows the values of the recoveries of microbial cell based on the experimental data and the parameters used in the numerical calculations. In this study, the recovery was defined by $(W_{out}/W_{in}) \times 10^2$, where W_{out} is the cell number in the effluent until the dimensionless time $T = 4$, and W_{in} is the total cell number inputted into the packed bed. The detachment rate-coefficient was zero for each case. This means that the cells attached once do not detach from the solid glass beads, under the conditions of this study.

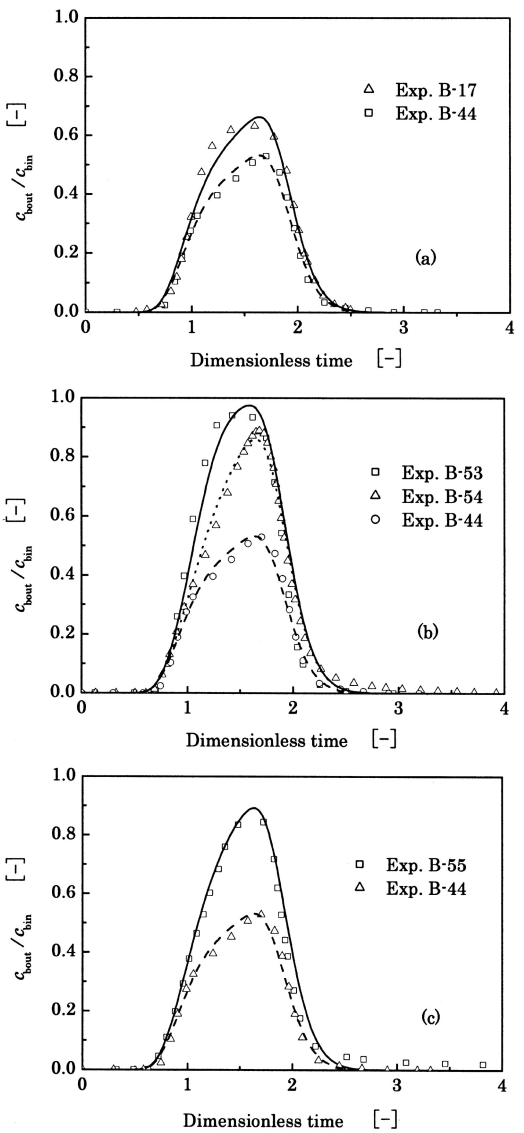

Fig. 4 Comparison of experimental breakthrough curves with calculated results (the solid line, broken line and dotted line : the calculation results.) (a): Breakthrough curves with a similar ratio of flow velocity to the input concentration. (□: B-44, and △: B-17); (b) : Breakthrough curves with different flow velocities. Flow velocity were 3.2×10^{-5}m s^{-1} (○: B-44), 6.5×10^{-5}m s^{-1}(△: B-54) and 1.3×10^{-4}m s^{-1}(□: B-53), and the cell-input concentrations were constant at 2.4×10^{14} cells m^{-3}, (c) : Breakthrough curved with different cell-input concentrations of 2.4×10^{14} cells m^{-3} (△: B-44) and 4.4×10^{14} cells m^{-3}(□: B-55), but a constant flow velocity of 3.2×10^{-5}m s^{-1}.

Table 2 Recovery of cell and parameters used in numerical model calculation

Run number	Recovery	Parameters						
		R_a [-]	K_a [-]	K_y [-]	$C_{s_{max}}$ [-]	k_a [s^{-1}]	k_y [s^{-1}]	$c_{s_{max}}$ [cell m^{-3}]
B-44	49.8%	0.12	1.0	0	0.94	1.33×10^{-4}	0	2.26×10^{14}
B-54	77.7%	0.06	1.6	0	0.26	4.33×10^{-4}	0	0.62×10^{14}
B-53	86.5%	0.03	4.0	0	0.10	21.7×10^{-4}	0	0.24×10^{14}
B-55	81.2%	0.21	0.2	0	2.00	2.67×10^{-5}	0	8.80×10^{14}
B-17	64.3%	0.14	0.6	0	0.70	1.63×10^{-4}	0	4.80×10^{14}

Fig. 4 (a) shows the breakthrough curves ($c_{b_{out}}/c_{b_{in}}$) for a similar ratio of the cell-input concentration to flow velocity in the range of from 0.75×10^{19} to 0.98×10^{19}. Here $c_{b_{out}}$ is the cell-concentration at the outlet of the packed bed. From the definition equation of R_a (equation (9b)), the value is directly proportional to the ratio of the cell-input concentration, $c_{b_{in}}$, to the flow velocity, v_{in}. Therefore, the responses may be the same if the ratio is fixed[22]. However, as shown in Fig. 4 (a), while these responses have relatively close tendency in comparison with the other run Nos. 53, 54, and 55, the responses of B-17 and B-44 show different recoveries, i.e., 64.3% for B-17 and 49.8% for B-44. This tendency suggests that the microbial transport appreciably depends on the flow velocity.

Fig. 4 (b) shows a comparison of the breakthrough curves for different flow velocities (B-44, B-54 and B-53). In these experiments, the cell-input concentrations were constant, 2.4×10^{14} cells m^{-3}, but the flow velocities were different, i.e., 3.2×10^{-5} m s^{-1} for B-44, 6.4×10^{-5} m s^{-1} for B-54 and 1.3×10^{-4} m s^{-1} for B-53. As shown in this figure, the breakthrough curves indicate strong dependency on the flow velocity. The peak height for B-53 was about two times higher than that for B-44. In addition, the shapes or slopes of the left shoulders of these curves were different; that is, the left shoulder was higher for the faster flow velocity. Table 2 shows that the recoveries, the attachment rate-coefficients and the maximum retention capacity are quite different for different flow velocities. The cell recovery increases with an increase of the flow velocity, while the attachment rate-coefficient and the maximum retention capacity decrease.

Fig. 4 (c) shows a comparison of the experimental data for different cell-input concentrations, 2.4×10^{14} cells m^{-3} for B-44 and 4.4×10^{14} cells m^{-3} for B-55, but a constant flow velocity of 3.2×10^{-5} m s^{-1}. The values of the dimensionless parameters of the attachment rate-coefficient and the maximum retention capacity used in the numerical calculation for the best fit were 1.0 and 0.94 for B-44, and 0.2 and 2.00 for B-55. For an increase in the cell-input concentration of up to about 1.8 times, the value of the attachment rate-coefficient decreased to about a quarter and the maximum retention capacity also increased to about two times, respectively. Further, the recoveries were 81.2% at the cell-input concentration of 4.4×10^{14} cells m^{-3} (B-55) and 49.8% at that of 2.4×10^{14} cells m^{-3} (B-44). Thus, the attachment rate and the retention of microbes depended on the cell-input concentration as well as the flow velocity.

To examine the attachment or retention capacity, a series of adsorption experiments under a stationary condition were carried out. In these batch experiments, glass beads (50-90 g, 1 mm diameter) and suspensions with various cell concentrations of about 100 ml were mixed. Based on the Langmuir equation, the values of the maximum absorption amount $c'_{s_{max}}$ and the absorption coefficient ($=k_y / k_a$) were obtained as 1.1×10^{15} cells m^{-3} and 1.25×10^{-9}, respectively. However, the maximum retention capacity $c_{s_{max}}$ obtained from the two-dimensional packed bed and the maximum adsorption amount $c'_{s_{max}}$ from the batch tests were different. (The value of $c_{s_{max}}$ for each run was always smaller than that of $c'_{s_{max}}$.) Thus, we must recognize the value of $c'_{s_{max}}$ obtained from the batch tests as a reference parameter used only to estimate the degree of cell retention due to the attachment of microbes on a solid.

Fig. 5 shows the results of this study and the data reported by Tan *et al.*[8]. Although the microbes, solid

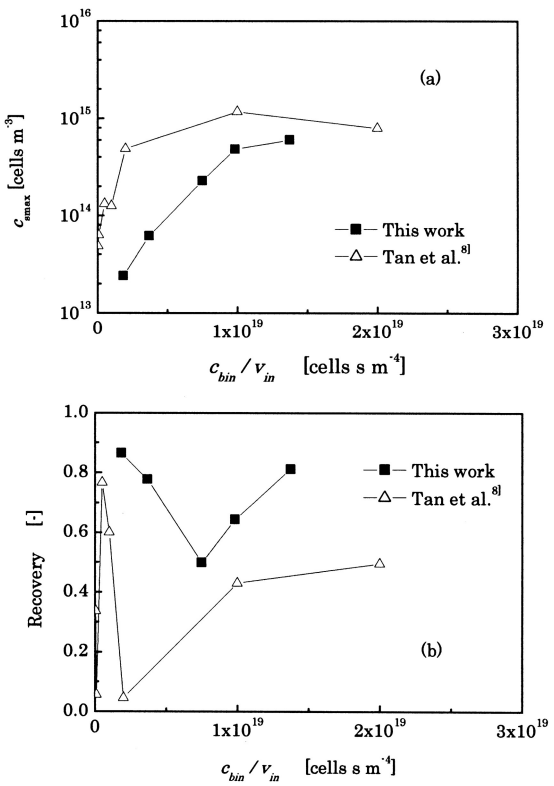

Fig. 5 Relationship between the number of microbes retained in porous media and the ratio of the cell-input concentration to the flow velocity. Microbes, solid and solution used in this experiment reported by Tan *et al.*[8] were *Pseudomonas* sp. strain KL2, an aquifer sand (90.3% of sand particle were 0.5-2.0 mm in size) and distilled water, respectively. (a) : the relation between the maxmum retention capacity and the ratio. (b) : the relation between the cell recovery and the ratio.

and solutions used in each report are different, the change of c_{smax} or the cell recovery as a function of c_{bin}/v_{in} has the same pattern. That is, the value of c_{smax} increases with an increase of c_{bin}/v_{in}. On the other hand, the cell recovery decreased once but increased after some value of c_{bin}/v_{in} in each work.

In general, the suitable distribution of both microbes and its nutrients in a reservoir is necessary for improving the efficiency of MEOR. In this study, the maximum retention capacity and cell recovery may be used to determine the suitability of the distribution of microbes. That is, when the maximum retention capacity has a larger value or the cell recovery is small, a large amount of microbes will be retained in a relatively small area near the input well. (Conversely, if the value of the maximum retention capacity (or the cell recovery) is very small (or large), the cell concentration in the enforcement field may also become small.) On the basis of the tendencies of the changes shown in Fig. 5, it is necessary to select an optimal flow velocity for each cell-input concentration, although its optimal value does not always agree with that for one-dimensional flow system.

Thus far, we have discussed the two-dimensional transport of microbes in porous media using breakthrough experiments and numerical calculations. However, one of the key parameters, the Rayleigh number, R_a, for all of the considerations is limited to relatively small values from 0.03 through 0.16, because of experimental limitations such as the maximum collection concentration of the microbe and the minimum flow rate of the peristaltic pump. Generally, the flow condition of the inputted cell suspension including the medium is radial, and the cell-input concentration in the suspension is in the range of from 1×10^{14} cells m^{-3} through 1×10^{17} cells m^{-3}. Considering the larger value of the true Rayleigh number, we must determine the transport behavior of microbes in porous media.

Fig. 6 shows the comparisons of breakthrough curves based on the two-dimensional model for different Rayleigh numbers (buoyancy-effect). Here, in order to understand just only the buoyancy-effect on

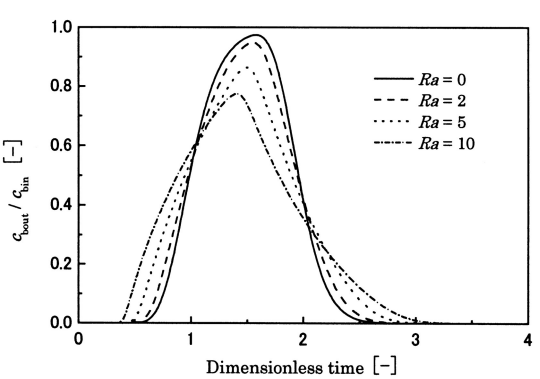

Fig. 6 Comparisons of numerical breakthrough curves for different Rayleigh numbers. In these numerical calculations, the Peclet number, the attachment and detachment rate-coefficients, and the maximum retention capacity were assumed to be constant, i.e., 50, 0.2, 5.0 and 2.0.

the breakthrough curves, the remaining parameters, i.e., the Peclet number, the attachment/detachment rate-coefficients and the maximum retention capacity, were assumed to be constant in these numerical calculations. As shown in Fig. 6, the transport and the distribution of microbes in porous media strongly depend also on the Rayleigh number (buoyancy-effect). When the value of the Rayleigh number is greater than 2.0, the buoyancy-effect on transport and distribution cannot be neglected, because of the density difference of cell suspension.

5. Conclusions

In order to understand the attachment behavior of microbes in the flow system of porous media, this study examined the relation of the attachment amount and the fluid flow velocity considering the injection concentration of cell suspension, in a vertical, two-dimensional packed bed (plate-type packed bed). The experimental data showed good agreement with the simple 2D mathematical model which took in terms of the gravitation and the attachment of microbes. In the model, the attachment /detachment of microbes on a solid can be described by a Langmuir-type adsorption equation. The experimental results obtained from the 2D porous media revealed the strong dependency of the flow velocity and the cell-input concentration on the microbial transport. Moreover, Rayleigh number (buoyancy-effect) is also a key parameter controlling the distribution of microbes. However, even if the value of the Rayleigh number were fixed, the breakthrough curves did not always agree. Because, if the buoyancy effect was limited (i.e., Rayleigh number is smaller than 2.0), the experimental results showed an optimal value of the ratio of $c_{b_{in}}$ to v_{in}, for both the maximum attachment amount and the cell recovery. This suggests the necessity of two-dimensional analysis for more reliable design of MEOR, even if we select the operation saving the buoyancy effect resulting from the difference in cell concentration.

References

1) Van Hamme, J. D., Singh, A. and Ward, O.P., 2003 : Recent Advances in Petroleum Microbiology. *Microbiology and Molecular Biology Reviews*, **67** (4), 503–549.
2) Yang, Y.G., Niibori, Y., Inoue, C. and Chida, T., 1999 : Modeling of Growth and Transport of Bacteria in Porous Media. *Proc. of IASTED International Conference Applied Modelling and Simulation* (AMS'99), 589–594.
3) Sugai, Y., Hong, C., Chida, T. and Enomoto, H., 2004 : Numerical Experiments of MEOR with the microbe producing water-soluble polymer. *J. of Japanese Association for Petroleum Technology*, **69** (5), 563–573 (Japanese with English Abstract).
4) Bryant, R.S. and Douglas, J., 1988 : Evaluation of microbial systems in porous media for EOR. *SPE Reservoir Eng*., 489–495.
5) Crawford, R.L. and Crawford. D.L., 1996 : *Bioremediation: Principles and applications*. Cambridge University Press. New York.
6) Kim, S. and Corapcioglu, M. Y., 1996 : A kinetic approach to modeling bacteria-facilitated groundwater contaminant transport. *Water Resour. Res*., **32**, 321–331.
7) Lindqvist, R., Cho, J.S. and Enfield, C.G., 1994 : A kinetic for cell density bacterial transport in porous media. Water Resour. Res., **30**, 3291-3299.
8) Tan, Y., Gannon, J.T., Baveye, P. and Alexander, M., 1994 : Transport of bacteria in an aquifer sand: Experiments and model simulations. *Water Resour. Res*., **30**, 3243–3252.
9) McCaulou, D.R. and Bales, R.C., 1995 : Effect of temperature-controlled motility on transport of bacteria and micro-sphere through saturated sediment. *Water Resour. Res*., **31**, 271–280.
10) Bengtsson, G. and Lindqvist, R., 1995 : Transport of soil bacteria controlled by density-dependent sorption kinetics. *Water Resour. Res*., **31**, 1247–1256.
11) Sarkar, A.K., Georgiuou, G. and Sharma M.M., 1994 : Transport of bacteria in porous media: I. An experimental investigation. *Biotechnol. Bioeng*., **44**, 489-497.
12) Sarkar, A.K., Georgiuou, G. and Sharma, M.M., 1994 : Transport of bacteria in porous media:II. A model for connective transport and growth. *Biotechnol. Bioeng*., **44**, 499–508.
13) Taylor, S.W. and Jaffe, P.R., 1990 : Substrate and biomass transport in a porous medium. *Water Resour. Res*., **26**, 2181–2194.

14) Vandevivere, P. and Baveye, P., 1992：Relationship between transport of bacteria and their clogging efficiency in sand columns. *Applied and Environ. Microbiol.*, **28**, 2523−2530.
15) Vandevivere, P., Baveye, P., Lozada, D.S. and DeLeo, P., 1995：Microbial clogging of saturated soils and aquifer materials: Evaluation of mathematical models. *Water Resour. Res.*, **31**, 2173−2180.
16) Shonnard, D.R., Taylor, R.T. and Hanna, M.L., 1994：Injection-attachment of Methylosinus trichosporium OB3b in a two-dimensional miniature sand-filled aquifer simulator. *Water Resour. Res.*, **30**, 25−35.
17) Sugai, Y., Hong, C., Ikeda, S., Chida, T., Enomoto, H. and Yazawa, N., 2002：Screening of water-soluble polymer producing microorganisms for MEOR. *J. of Japanese Association for Petroleum Technology*, **67** (3), 277−286 (Japanese with English Abstract).
18) Sugai, Y., Hong, C., Chida, T. and Enomoto, H., 2004：Simulation study on the performance and mechanism of MEOR with a water-soluble polymer producing microbe. *J. of Japanese Association for Petroleum Technology*, **69** (4), 335−347 (Japanese with English Abstract).
19) Yonebayashi, H., Hong, C., Kishita, A., Enomoto, H. and Chida, T., 1996：Fundamental studies on MEOR with anaerobes : Evaluation of activities of isolated anaerobes. *J. of Japanese Association for Petroleum Technology*, **61** (5), 443−451 (Japanese with English Abstract).
20) Corapcioglu, M.Y. and Haridas, A., 1984：Transport and fate of microorganisms in porous media: A theoretical investigation. *J. Hydrology*. **72**, 149−169.
21) Corapcioglu, M.Y. and Haridas, A., 1985：Microbial transport in soils and groundwater: A numerical model. *Adv. Water Resour.*, **8**, 188−200.
22) Yang, Y.G., Niibori, Y. and Chida, T., 1998：Laboratory experiments and numerical analyses on nutrients transport for MEOR. *J. of Japanese Association for Petroleum Technology*, **63** (3), 229−238 (Japanese with English Abstract).
23) Haga, D., Niibori, Y. and Chida, T., 1999：Hydrodynamic dispersion and mass transfer in unsaturated flow. *Water Resour. Res.*, **35**, 1065−1077.
24) Levenspiel, O., 1972：*Chemical Reaction Engineering* 2nd ed. JOHN WILEY & SONS, New York, p 253−283.

要　　旨

MEOR 設計のための多孔質体における微生物付着と移動に関する基礎的研究

楊　延国・新堀雄一・井上千弘・千田　佶

固相表面に付着する微生物の菌体数は液相に存在する浮遊菌より大きいことが知られている。MEOR において微生物の活動を効率化するためには，貯留層の対象空間おいて微生物の付着量を大きくする必要がある。本研究では，流動を伴う場合の微生物の付着挙動を理解するために，垂直二次元の多孔質体を平行平板の充填層により表し，そのなかにおける微生物の付着挙動と流体流速との関係について調べた。

微生物は化学走性および自走性のない微生物として乳酸桿菌を用い，栄養塩を制限し増殖のない条件とした。実験では，微生物の懸濁液を所定時間，所定流量にて多孔質体に注入した。微生物懸濁液の注入後，蒸留水により押し流し，流出する微生物濃度の変化を濁度により連続的に定量化した。得られた流出微生物濃度を比較的簡便な二次元の数学モデルにより解析した。数学モデルは移流項，分散項および付着項を含み，浮力の効果も考慮した。付着項にはこれまで多く適用されてきたラングミュアー型の速度式を用いた。

実験結果より，注入したすべての微生物が流出するのではなく，一部の微生物は固相に付着することを確認した。注入した微生物量に対する流出した微生物量を流出率として定義した。また，数学モデルによる解析から微生物の固相への見かけの最大付着量を評価した。微生物は注入濃度および注入流速によって，最大付着量は異なり，流出率も変化した。注入流速に対する注入微生物量の比は，それらを整理する１つのパラメータである。実験結果は，その比に最大付着量と流出率について最適な値が存在することを示した。このことは，仮に菌体濃度差による浮力の効果を抑制するオペレーションを選んだとしても，MEOR の設計精度向上に対する二次元解析の必要性を示唆している。